



# Multinuclear Metal-Binding Ability of the N-Terminal Region of Human Copper Transporter Ctr1: Dependence Upon pH and Metal Oxidation State

Maria Incoronata Nardella<sup>1</sup>, Mariagrazia Fortino<sup>2</sup>, Alessandra Barbanente<sup>1</sup>, Giovanni Natile<sup>1</sup>, Adriana Pietropaolo<sup>2</sup> and Fabio Arnesano<sup>1\*</sup>

## OPEN ACCESS

### Edited by:

Simone Ciofi Baffoni,  
University of Florence, Italy

### Reviewed by:

David Huffman,  
Western Michigan University,  
United States  
Nicola d'Amelio,  
University of Picardie Jules Verne,  
France

### \*Correspondence:

Fabio Arnesano  
fabio.arnesano@uniba.it

### Specialty section:

This article was submitted to  
Cellular Biochemistry,  
a section of the journal  
Frontiers in Molecular Biosciences

Received: 16 March 2022

Accepted: 20 April 2022

Published: 05 May 2022

### Citation:

Nardella MI, Fortino M, Barbanente A, Natile G, Pietropaolo A and Arnesano F (2022) Multinuclear Metal-Binding Ability of the N-Terminal Region of Human Copper Transporter Ctr1: Dependence Upon pH and Metal Oxidation State. *Front. Mol. Biosci.* 9:897621. doi: 10.3389/fmolb.2022.897621

<sup>1</sup>Department of Chemistry, University of Bari Aldo Moro, Bari, Italy, <sup>2</sup>Dipartimento di Scienze Della Salute, University of Catanzaro, Catanzaro, Italy

The 14mer peptide corresponding to the N-terminal region of human copper transporter Ctr1 was used to investigate the intricate mechanism of metal binding to this plasma membrane permease responsible for copper import in eukaryotic cells. The peptide contains a high-affinity ATCUN Cu(II)/Ni(II)-selective motif, a methionine-only MxMxxM Cu(I)/Ag(I)-selective motif and a double histidine HH(M) motif, which can bind both Cu(II) and Cu(I)/Ag(I) ions. Using a combination of NMR spectroscopy and electrospray mass spectrometry, clear evidence was gained that the Ctr1 peptide, at neutral pH, can bind one or two metal ions in the same or different oxidation states. Addition of ascorbate to a neutral solution containing Ctr1<sub>1-14</sub> and Cu(II) in 1:1 ratio does not cause an appreciable reduction of Cu(II) to Cu(I), which is indicative of a tight binding of Cu(II) to the ATCUN motif. However, by lowering the pH to 3.5, the Cu(II) ion detaches from the peptide and becomes susceptible to reduction to Cu(I) by ascorbate. It is noteworthy that at low pH, unlike Cu(II), Cu(I) stably binds to methionines of the peptide. This redox reaction could take place in the lumen of acidic organelles after Ctr1 internalization. Unlike Ctr1<sub>1-14</sub>-Cu(II), bimetallic Ctr1<sub>1-14</sub>-2Cu(II) is susceptible to partial reduction by ascorbate at neutral pH, which is indicative of a lower binding affinity of the second Cu(II) ion. The reduced copper remains bound to the peptide, most likely to the HH(M) motif. By lowering the pH to 3.5, Cu(I) shifts from HH(M) to methionine-only coordination, an indication that only the pH-insensitive methionine motif is competent for metal binding at low pH. The easy interconversion of monovalent cations between different coordination modes was supported by DFT calculations.

**Keywords:** Ctr1, copper, silver, metal transport, redox processes, NMR spectroscopy, mass spectrometry, DFT calculations

## INTRODUCTION

An elaborate machinery controls the numerous metal ions circulating in the blood and stored in the cells of living organisms. The intracellular concentration of these metal ions is finely regulated because, despite their beneficial effects, they are potentially toxic (particularly those redox active) and can participate in aberrant reactions.

In the case of copper (Cu), the metal participates in various cellular metabolic processes, such as oxidative phosphorylation (Hu et al., 1977; Tsukihara et al., 1995), formation of connective tissue (Kagan and Li, 2003), iron metabolism (Dancis et al., 1994), maturation of neuropeptides (Prigge et al., 2000), detoxification of free radicals (Baker et al., 2017), pigmentation (Matoba et al., 2006), etc. To sustain copper demand, while minimizing the risk of toxic side effects, is critically important for cell viability. For this reason the homeostasis of Cu(I) is finely controlled by a complex protein system, which keeps the metal ion protein-bound while it is delivered to the various intracellular compartments, so preventing the toxic effects stemming from intracellular accumulation of unbound Cu(I) species (O'Halloran and Culotta, 2000; Huffman and O'Halloran, 2001; Field et al., 2002; Boal and Rosenzweig, 2009; Robinson and Winge, 2010; Nevitt et al., 2012; Palumaa, 2013; Lutsenko, 2021). The copper transporter 1 (Ctr1) is a protein essential for copper transport across the plasma membrane (Dancis et al., 1994; Lee et al., 2001). Human Ctr1 (hCtr1) is a membrane protein of approximately 28 kDa and made of 190 amino acids, which features three transmembrane  $\alpha$ -helices, a C-terminal domain of 15 amino acids and a long N-terminal extracellular domain (ectodomain) of 67 amino acids (Zhou and Gitschier, 1997; Pope et al., 2012). The exact mechanism by which copper enters the cell is not entirely elucidated, however experimental evidence indicates that three units of Ctr1 are associated to form a pore acting as an ion channel (De Feo et al., 2009; Ren et al., 2019). The localization of Ctr1 is controlled by the intra and extra-cellular copper concentration. An increase in the extracellular concentration of copper induces endocytosis of Ctr1, so reducing the transit of the metal ion across the membrane (Petris et al., 2003; Guo et al., 2004; Van Den Berghe et al., 2007). Conversely, a decrease in copper concentration restores the Ctr1 level at the plasma membrane (Molloy and Kaplan, 2009; Clifford et al., 2016). Proteins homologous to Ctr1 transport selectively the Cu(I) ions, while in the extracellular environment the metal is present mainly in the oxidized Cu(II) form. Therefore, the intervention of reducing agents or enzymes capable of transforming Cu(II) into Cu(I) is required before the metal can be transported into the cytosol. In the case of yeast *S. cerevisiae*, two selective reductases for copper and iron are present (Fre1 and Fre2) (Hassett and Kosman, 1995; Georgatsou et al., 1997). In humans, there is a family of proteins, called STEAP, capable of reducing the two metal ions and facilitate their acquisition by cells (Ohgami et al., 2006; Oosterheert et al., 2018). An alternative, simplified, copper reduction model has also been proposed. It is based on the observation that the N-terminal end of hCtr1 is able to bind and reduce Cu(II) to Cu(I) using ascorbate, and to stabilize Cu(I)

thanks to the presence of histidine (His) and methionine (Met) motifs in monomeric (Pushie et al., 2015) or multimeric (Galler et al., 2020) arrangements. The binding of Cu(I) to hCtr1 induces a conformational change, which promotes the interaction of the ectodomain with the cell membrane and may represent the initial step of the Cu(I) uptake process (Yang et al., 2019).

In the present study, we investigated the metal binding properties of a 14mer peptide corresponding to the first 14 amino acids of the N-terminal region of human Ctr1 (Ctr1<sub>1-14</sub>). The peptide contains the amino acid motifs essential for the acquisition of copper from the extracellular environment. The initial H<sub>2</sub>N-X<sub>2</sub>-His motif (known as the ATCUN motif) is also found in human serum albumin (HSA) and is selective for Cu(II) and Ni(II) (Bossak et al., 2018; Gonzalez et al., 2018). Cu(II) binds to this site in a square planar coordination geometry involving four nitrogen atoms (4N): the free NH<sub>2</sub> terminus, a histidine residue in the third position and the two intervening amidic nitrogens (Santoro et al., 2018).

In the N-terminal region, both hCtr1 and yeast Ctr1 (yCtr1) exhibit Met-rich motifs MxM and MxxM, able to bind Cu(I) (Jiang et al., 2005; Rubino et al., 2010). Furthermore, hCtr1, unlike yCtr1, contains also histidine-rich motifs that have been implicated in the acquisition of Cu(II) and Cu(I) in mammals (Haas et al., 2011). In particular, quite close to the N-terminal end of hCtr1 there is a bis-His (HH) motif (Himes et al., 2007; Shearer and Szalai, 2008) flanked by a Met (the HHM motif) capable of binding and stabilizing Cu(I) (Pushie et al., 2015). The contiguous presence of ATCUN and HHM motifs suggests a possible interaction with copper in both oxidation states (Haas et al., 2011; Pushie et al., 2015).

Based on the above consideration, we deemed it appropriate to investigate the interaction of Ctr1<sub>1-14</sub> with copper in both oxidation states and also with the redox-inactive Ag(I) ion, as a Cu(I) mimic. Moreover, since the endosomal compartment where hCtr1 is internalized is acidic, the investigation was carried on at different pH values (from neutral to highly acidic).

## MATERIALS AND METHODS

The 14mer Ctr1<sub>1-14</sub> peptide (sequence MDHSHHMGMSYMDS, MM: 1665.85 Da; pI: 5.68) was purchased from Genscript Biotech (Piscataway, New Jersey, United States) and used without further purification.

### Nuclear Magnetic Resonance (NMR) Spectroscopy

NMR samples were prepared by dissolving Ctr1<sub>1-14</sub> in phosphate buffer (Pi, 25 mM, pH = 7 or 3.5) or in 2-(N-morpholino) ethanesulfonic acid (MES, 10 mM, pH = 7) at 250  $\mu$ M concentration. NMR titrations were performed by gradually adding CuSO<sub>4</sub> or AgNO<sub>3</sub> dissolved in pure water to the apopeptide solution, directly in the NMR tube. 1D <sup>1</sup>H NMR spectra were recorded at 298 K on a Bruker Avance 300 Ultrashield spectrometer equipped with a double resonance broad-band probe with Z-Gradient. 1D <sup>1</sup>H NMR spectra were

acquired with a relaxation delay of 1.5 s, 256 scans, 32K data points and a spectral width of 16 ppm.  $^1\text{H}$  chemical shifts were referenced to trimethylsilylpropanoic acid (TSP,  $\delta_{1\text{H}} = 0.0$  ppm).

## Electrospray Ionization Mass Spectrometry (ESI-MS)

Solutions of Ctr1<sub>1-14</sub> (200  $\mu\text{M}$ ) and its adducts with Cu(II) and Ag(I), at different metal:peptide ratios, were prepared in  $\text{NH}_4\text{OAc}$  (20 mM) at 25 °C. Aliquots of these samples were diluted with buffer to a final concentration of 20  $\mu\text{M}$  and directly infused into the mass spectrometer, an Agilent 6530 Accurate-Mass Quadrupole Time-of-Flight (Q-TOF) system equipped with an electrospray interface. Ionization was achieved in the positive or negative ion mode by application of 4.0 kV at the entrance of the capillary; the pressure of the nebulizer gas was 20 psi. The drying gas was heated to 325 °C and introduced at a flow rate of 10  $\mu\text{L}/\text{min}$ . Full-scan mass spectra were recorded in the mass/charge ( $m/z$ ) range of 50–3,000. Isotopic distributions were calculated with the program Molecular Weight Calculator (<https://omics.pnl.gov/software/molecular-weight-calculator>).

## Modeling Calculations

The initial coordinates of the Ctr1<sub>1-14</sub> peptide were obtained using the CHIMERA software (Pettersen et al., 2004). The coordinates were energy minimized through the Steepest Descent Algorithm and equilibrated with 9 ns of standard molecular dynamics at 300 K using the amber99SB force field (Ivani et al., 2016) and the TIP3P potential (Jorgensen et al., 1983) for water molecules, within the GROMACS MD code - version 2020.2 (Abraham and van der Spoel, 2020). Parallel Bias Metadynamics (PBMetaD) (Pfaendtner and Bonomi, 2015) simulations were subsequently performed using the GROMACS MD code - version 2020.2 (Abraham and van der Spoel, 2020) in the NVT ensemble, using the gyration radius as collective variable. Gaussians with initial height equal to 1.2 kJ/mol and width of 0.2 nm were deposited with a bias factor equal to 20. The total time of the simulation was 45 ns.

The three highly populated conformers were extracted from the PBMetaD trajectory through cluster analysis using the method of Daura and van Gunsteren (Daura et al., 1999) and were used as starting coordination geometries. The coordination models of Ctr1<sub>1-14</sub> with Ag(I) were built considering the residues from Met1 to Met12 and capping the side chains of Asp2, Ser4, Ser10, Tyr11, Asp13 and Ser14 with hydrogen atoms to reduce the computational cost and maintain simulation accuracy. The derived coordinates were optimized at *ab initio* level, within the Density Functional Theory (DFT) framework by using the PBE functional, suitable for this type of systems (Ernzerhof and Perdew, 1998) and the DGDZVP basis sets (Godbout et al., 1992) with Gaussian16 (Frisch et al., 2016) suite of quantum chemical programs. The use of double-zeta DGDZVP basis set allows to combine a high computational speed and a high accuracy for the study of large systems (Siiskonen and Priimagi, 2017).

## RESULTS

### Analysis of Ctr1<sub>1-14</sub> at Neutral and Acidic pH

The Ctr1<sub>1-14</sub> apo-peptide was initially characterized by electrospray ionization mass spectrometry (ESI-MS) to verify its identity and degree of purity. The ESI-MS spectrum carried out in  $\text{NH}_4\text{OAc}$  shows two main signals with  $m/z$  ratios of 833.3012 and 555.8680, associated to the doubly and triply charged species, respectively (Supplementary Figure S1; Table 1).

Subsequently, a 1D  $^1\text{H}$  NMR spectrum of the apo-peptide was recorded in 10 mM MES at pH 7.0 (Supplementary Figure S2) and in 25 mM Pi buffer at pH 7.0 and 3.5 (Figure 1). The main spectral changes between neutral and acidic pH were observed in the region of amides and aromatic protons. While the strong degenerate signal assigned to the  $\epsilon\text{-CH}_3$  methyl protons of the four Met residues and the two signals of Tyr phenyl ring were nearly insensitive to the pH variation; in contrast, the signals of the His imidazole ring were highly perturbed. This result is in agreement with the protonation of imidazole nitrogen ( $\text{pK}_a \sim 6$ ) in the pH range from 7.0 to 3.5, and suggests that metal ions may prefer different coordination modes depending upon the neutral or acidic environment in which the protein is placed.

Structural models of apoCtr1<sub>1-14</sub> were obtained through Parallel Bias Metadynamics (PBMetaD) (Pfaendtner and Bonomi, 2015) simulations. The main clusters of conformers extracted from the PBMetaD trajectory, representing three possible metal coordination networks, are highlighted in Figure 2. The first cluster is characterized by a close proximity of Met7, Met9 and Met12 and represents a population of 84% (Figure 2A). The second cluster features a network of residues involving His5, Met7 and Met12 and is 10% populated (Figure 2B). Finally, the third cluster features a close proximity of His5, His6 and Met7 and represents a population of 6% (Figure 2C). In the last cluster, a  $\beta$ -turn component of the secondary structure was found between His6 and Met7 residues.

### Interaction of Ctr1<sub>1-14</sub> With Cu(II) Ions

The interaction between Cu(II) and Ctr1<sub>1-14</sub> was investigated via NMR by treating the peptide solution (250  $\mu\text{M}$ ) with increasing aliquots of a solution of  $\text{CuSO}_4$ , up to 1 eq of Cu(II), both in 25 mM Pi and in 10 mM MES buffers at pH 7.0 (Figure 3). In Pi, the Cu(II) ion binds to Ctr1<sub>1-14</sub> and, given its paramagnetic nature, determines the broadening of the  $^1\text{H}$  NMR signals, in particular those of the His ring which show the greatest relative reduction in intensity. Moreover, the addition of Cu(II) produces only a negligible dipolar hyperfine (pseudocontact) shift, which is consistent with a type-II Cu(II) site (ATCUN) having modest magnetic susceptibility anisotropy (Arnesano et al., 2005). In MES, the broadening of the peptide signals was larger than that observed in the titration carried out in Pi buffer. This can be explained with the poorer coordinating ability of MES with respect to phosphate, which makes more Cu(II) available for binding to the peptide.

The interaction between Cu(II) and the peptide was also monitored by ESI-MS. Two signals were observed at 864.7583

**TABLE 1** | Stoichiometry of Ctr1<sub>1-14</sub> complexes with Cu(II) and Ag(I) ions observed by ESI-MS.

Ions	Experimental $m/z$ <sup>a</sup>	Calculated $m/z$ <sup>a</sup>	$\Delta Da$	Error (ppm)
<i>apo</i> Ctr1 <sub>1-14</sub>				
[Ctr1 <sub>1-14</sub> + 2H] <sup>2+</sup>	833.3012	833.2998	0.0014	2
[Ctr1 <sub>1-14</sub> + 3H] <sup>3+</sup>	555.8680	555.8692	-0.0012	-2
Ctr1 <sub>1-14</sub> -Cu(II)				
[Ctr1 <sub>1-14</sub> + Cu(II)] <sup>2+</sup>	864.7583	864.7618	-0.0035	-4
[Ctr1 <sub>1-14</sub> + Cu(II) + H] <sup>3+</sup>	576.8399	576.8438	-0.0039	-7
Ctr1 <sub>1-14</sub> -2Cu(II)				
[Ctr1 <sub>1-14</sub> + 2Cu(II) - 2H] <sup>2+</sup>	895.2160	895.2238	-0.0078	-9
[Ctr1 <sub>1-14</sub> + 2Cu(II) - H] <sup>3+</sup>	597.1451	597.1518	-0.0067	-11
Ctr1 <sub>1-14</sub> -Ag(I)				
[Ctr1 <sub>1-14</sub> + Ag(I) + H] <sup>2+</sup>	887.2496	887.2485	0.0011	1
[Ctr1 <sub>1-14</sub> + Ag(I) + 2H] <sup>3+</sup>	591.8346	591.8349	-0.0003	-1
Ctr1 <sub>1-14</sub> -2Ag(I)				
[Ctr1 <sub>1-14</sub> + 2Ag(I)] <sup>2+</sup>	940.1882	940.1971	-0.0089	-9
[Ctr1 <sub>1-14</sub> + 2Ag(I) + H] <sup>3+</sup>	627.1270	627.1340	-0.0070	-11
Ctr1 <sub>1-14</sub> -Ag(I),Cu(II)				
[Ctr1 <sub>1-14</sub> + Ag(I) + Cu(II) - H] <sup>2+</sup>	917.6949	917.7104	-0.0155	-17
[Ctr1 <sub>1-14</sub> + Ag(I) + Cu(II)] <sup>3+</sup>	612.1314	612.1429	-0.0115	-19

<sup>a</sup>The reported  $m/z$  ratios are referred to the prevailing isotopologue in the isotope pattern.

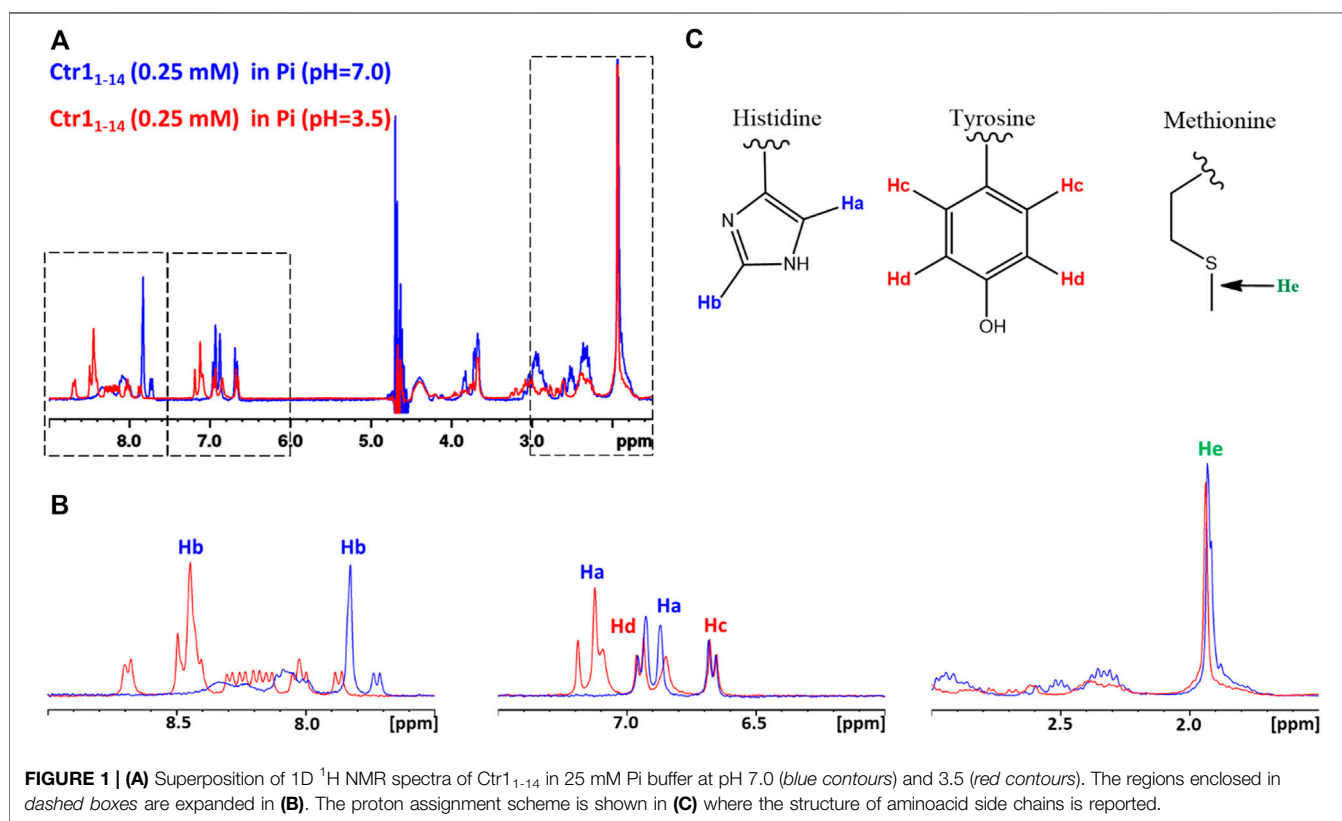
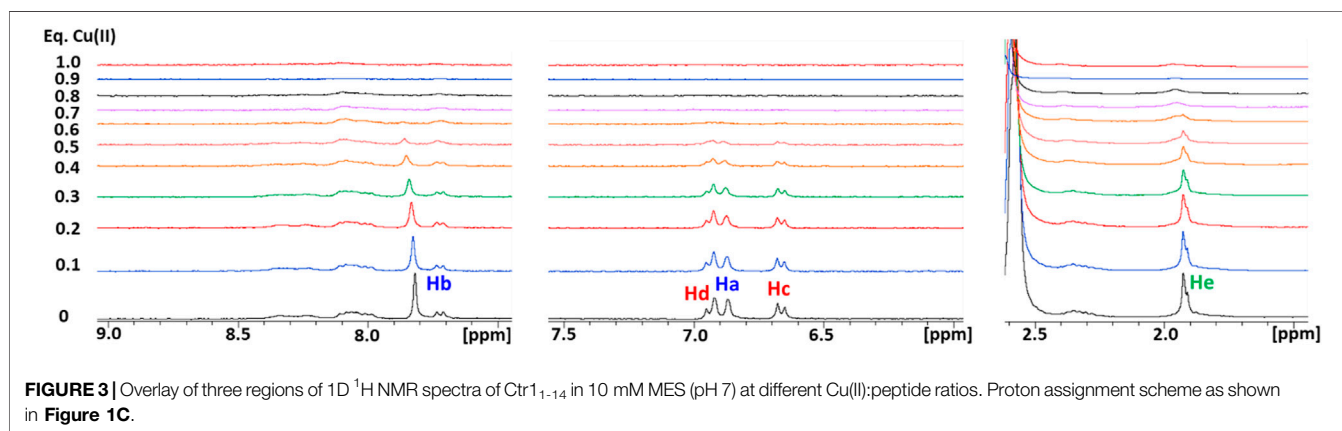
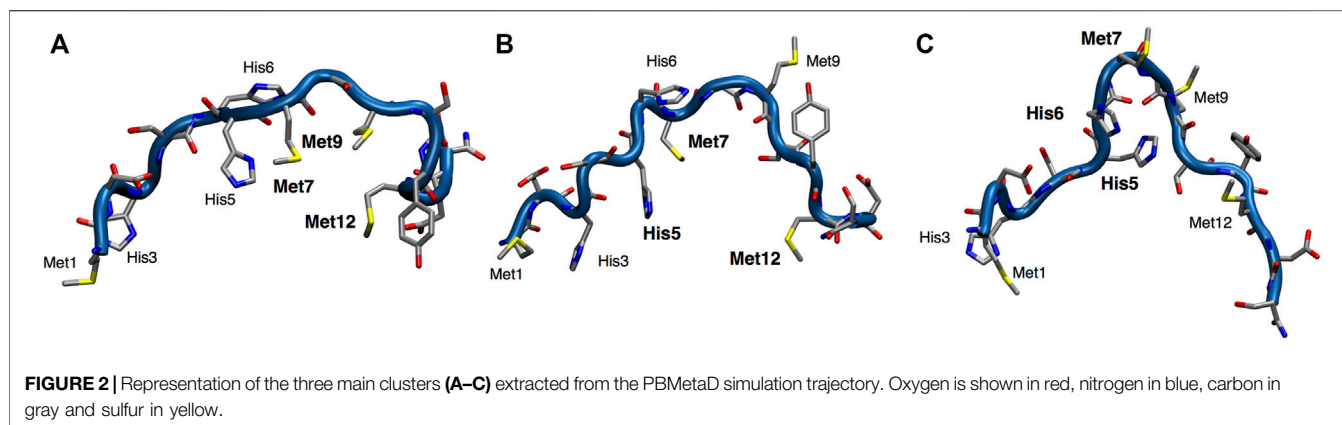


**FIGURE 1** | (A) Superposition of 1D <sup>1</sup>H NMR spectra of Ctr1<sub>1-14</sub> in 25 mM Pi buffer at pH 7.0 (blue contours) and 3.5 (red contours). The regions enclosed in dashed boxes are expanded in (B). The proton assignment scheme is shown in (C) where the structure of aminoacid side chains is reported.

and 576.8399  $m/z$ , corresponding to the adduct Ctr1<sub>1-14</sub>-Cu(II) having 2+ and 3+ overall charge, respectively (Figures 4A, B). The addition of Cu(II) beyond one equivalent leads to the almost complete disappearance of the NMR signals, however the ESI-MS spectra indicate the binding of a second Cu(II) ion to the peptide, as deduced from

the appearance of two signals at 895.2160 and 597.1451  $m/z$  (2+ and 3+ charged Ctr1<sub>1-14</sub>-2Cu(II) adduct) with the predicted isotopic distribution pattern (Figures 4C, D). The relative abundance of Ctr1<sub>1-14</sub> species (apopeptide and metal adducts) based on ESI-MS peak intensity at different Cu(II):peptide ratios is reported in panel E of Figure 4.



## Interaction of Ctr $_{1-14}$ With Ag(I) Ions

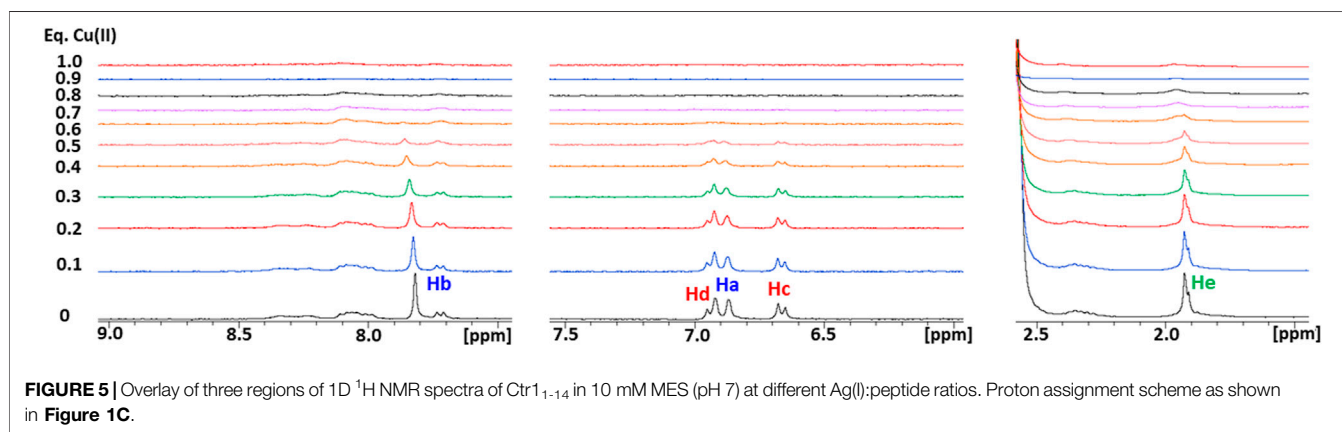
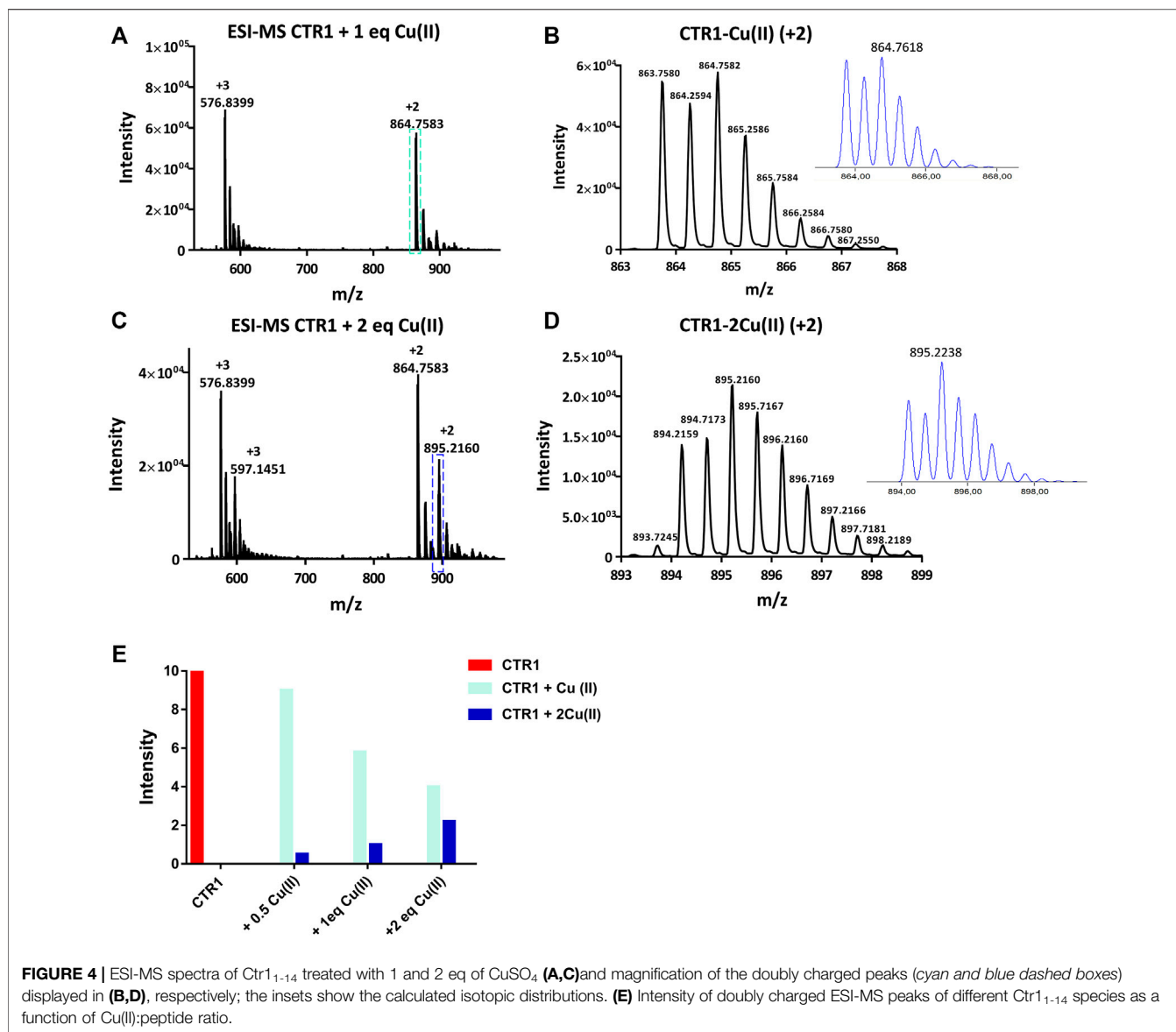
As a next step, the interaction of Ctr $_{1-14}$  with redox-stable Ag(I), as a mimic of Cu(I), was investigated via NMR. Thus, a peptide solution (250  $\mu\text{M}$ ) was treated with increasing aliquots of AgNO $_3$  both in Pi buffer (25 mM) and in MES (10 mM) at pH 7.0. NMR is more informative in the present case given the diamagnetic nature of the metal ion. Ag(I) was found to perturb the signals of His and Met, indicating the involvement of both types of residues in Ag(I) coordination. In particular, the methyl signals of methionines underwent a downfield shift with respect to the apo-peptide and a splitting into four peaks, indicating chemical inequivalence of  $\epsilon\text{-CH}_3$  groups. Similarly to Cu(II), also in this case a greater variation of chemical shifts was observed in MES buffer than in Pi. Chemical shift changes were complete after addition of 2 eq of Ag(I) to the peptide (**Figure 5**). Consistently, the ESI-MS spectra indicated the binding of one and two Ag(I) ions, giving rise to two pairs of signals at 887.2496 and 591.8346  $m/z$  and at 940.1882 and 627.1270  $m/z$ , respectively (in each pair the first signal belongs to the 2 + fragment and the second to the 3 + fragment; **Figures 6A–E**).

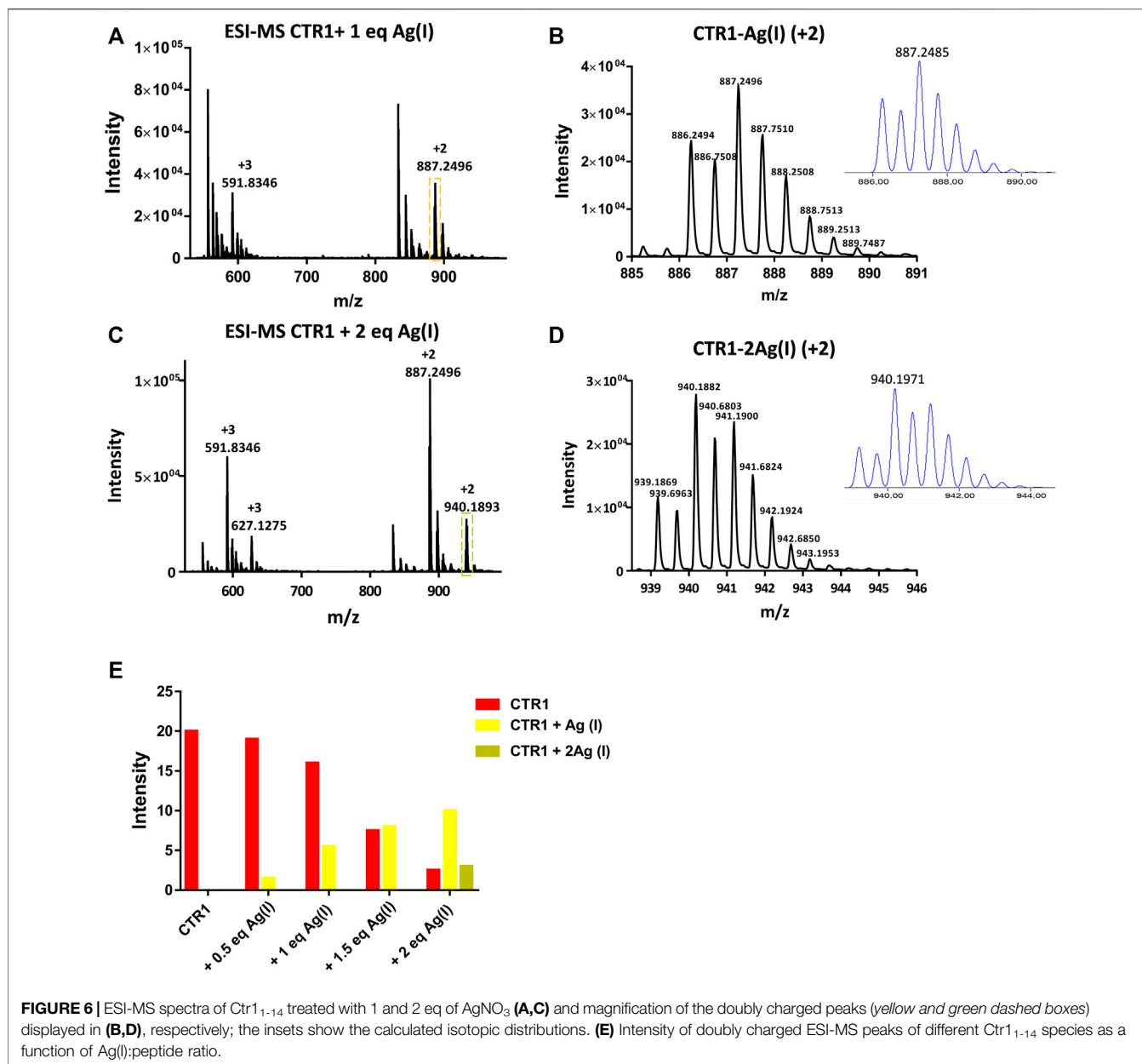
To model the putative metal binding site(s), the Ag(I) ion was coordinated to the network topologies calculated for the apo-peptide (see above), and the metal-bound coordinates were optimized at the Density Functional Theory (DFT) level using PBE as density functional (Ernzerhof and Perdew, 1998) and

DGDZVP as basis sets (Godbout et al., 1992). The DFT optimized structures of Ctr $_{1-14}$  coordinated to Ag(I) are reported in **Figure 7** and the coordination distances are listed in **Table 2**.

Model 1 shows a quasi-trigonal geometry around the Ag(I) ion which involves the sulfur atoms of Met7 and Met12 and the carbonyl of Met7, with a predicted hydrogen bond involving the amide proton and the sulfur atom of Met9 (it can be noted that this model alone could account for different chemical shifts for all methionine methyls). In Model 2, Ag(I) has a pseudo-tetrahedral geometry involving the N $\epsilon$ 2 of His5, the sulfur atom of Met12 and the two carbonyl groups of Ser10 and Tyr11. Model 3 is compatible with a quasi-tetrahedral geometry around the Ag(I) ion involving the N $\epsilon$ 2 of His5 and His6, the sulfur atom of Met7 and the carbonyl group of His6. In Model 4, Ag(I) has a pseudo-linear coordination geometry involving N $\epsilon$ 2 of His5 and His6, eventually bent by the hydrogen bonds between the imidazole ring proton HN $\delta$ 1 of His6 and the sulfur atom of Met7 and between HN $\delta$ 1 of His5 and the carbonyl oxygen of Ser10.

The calculated total energy differences are reported in **Table 3** and indicate that Model 1 is the lowest in energy, followed by Model 2 and Model 3 with energy differences of 0.47 and 0.82 kcal/mol, respectively. These small energy differences are easily accessible owing to thermal effects at room temperature and suggest a possible interconversion between different





coordination modes. Model 4 is predicted to be the highest in energy ( $\Delta E = +6.33$  kcal/mol).

### Simultaneous Binding of Cu(II) and Ag(I) to Ctr1<sub>1-14</sub>

Given the presence of multiple metal binding sites in Ctr1<sub>1-14</sub>, the possible interaction of the peptide with both Cu(II) and Ag(I) was investigated.

Addition of Cu(II) to a solution of Ctr1<sub>1-14</sub> containing 1 eq of Ag(I) in MES (pH 7.0), was found to cause a widespread broadening of the 1D <sup>1</sup>H NMR signals; however, at sub-stoichiometric Cu(II) addition a shift to lower fields of the methyl signals of methionines could be detected (**Figure 8**).

Since, apart from broadening, Cu(II) alone did not cause any significant shift of apo-peptide peaks (see **Figure 3**), the downfield shift of the  $\epsilon$ -CH<sub>3</sub> signals could indicate a further shift of Ag(I) coordination towards the methionines caused by the interaction of Cu(II) with histidines, whose signals undergo the largest line broadening due to the paramagnetic effect of Cu(II). It is concluded that Ctr1<sub>1-14</sub> can accommodate a Cu(II) (ATCUN site) and an Ag(I) ion. On the basis of the different Ag(I) coordination models discussed above and displayed in **Figure 7**, it can be proposed that the conformer with Met-only coordination (Model 1 in **Figure 7A**), which was already found to be the most favored in the interaction with the free peptide, can become even more populated after addition of Cu(II).

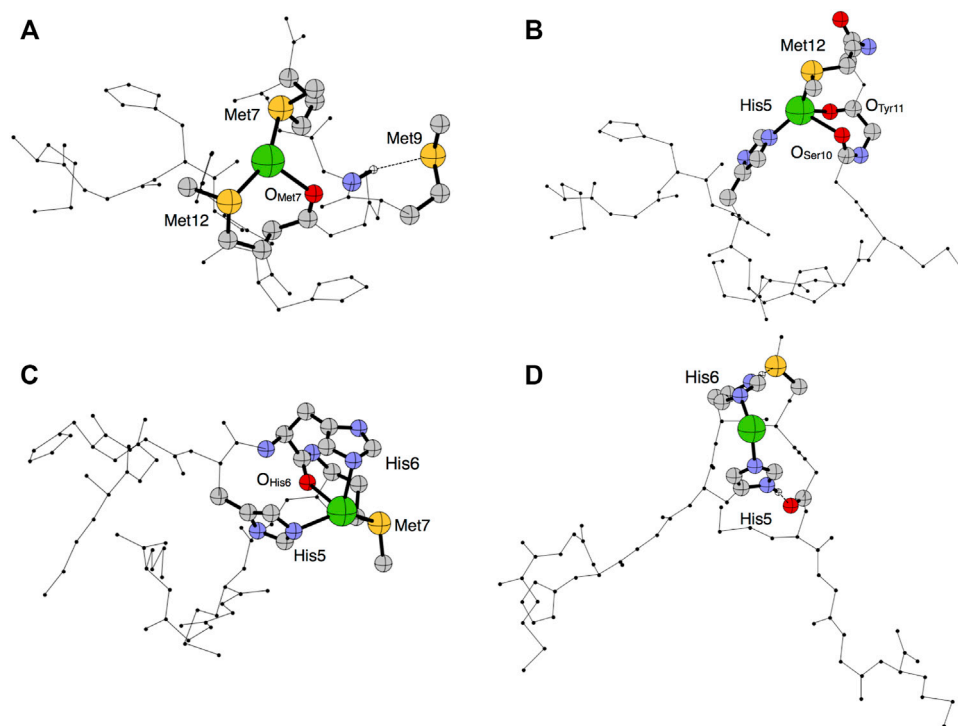


**FIGURE 7** | Optimized structural models 1–4 (**A–D**) predicted in the PBE/DGDZVP framework for Ag(I)-Ctr<sub>1-14</sub>. The silver ion is shown in green, oxygen in red, nitrogen in blue, carbon in grey and sulfur in yellow.

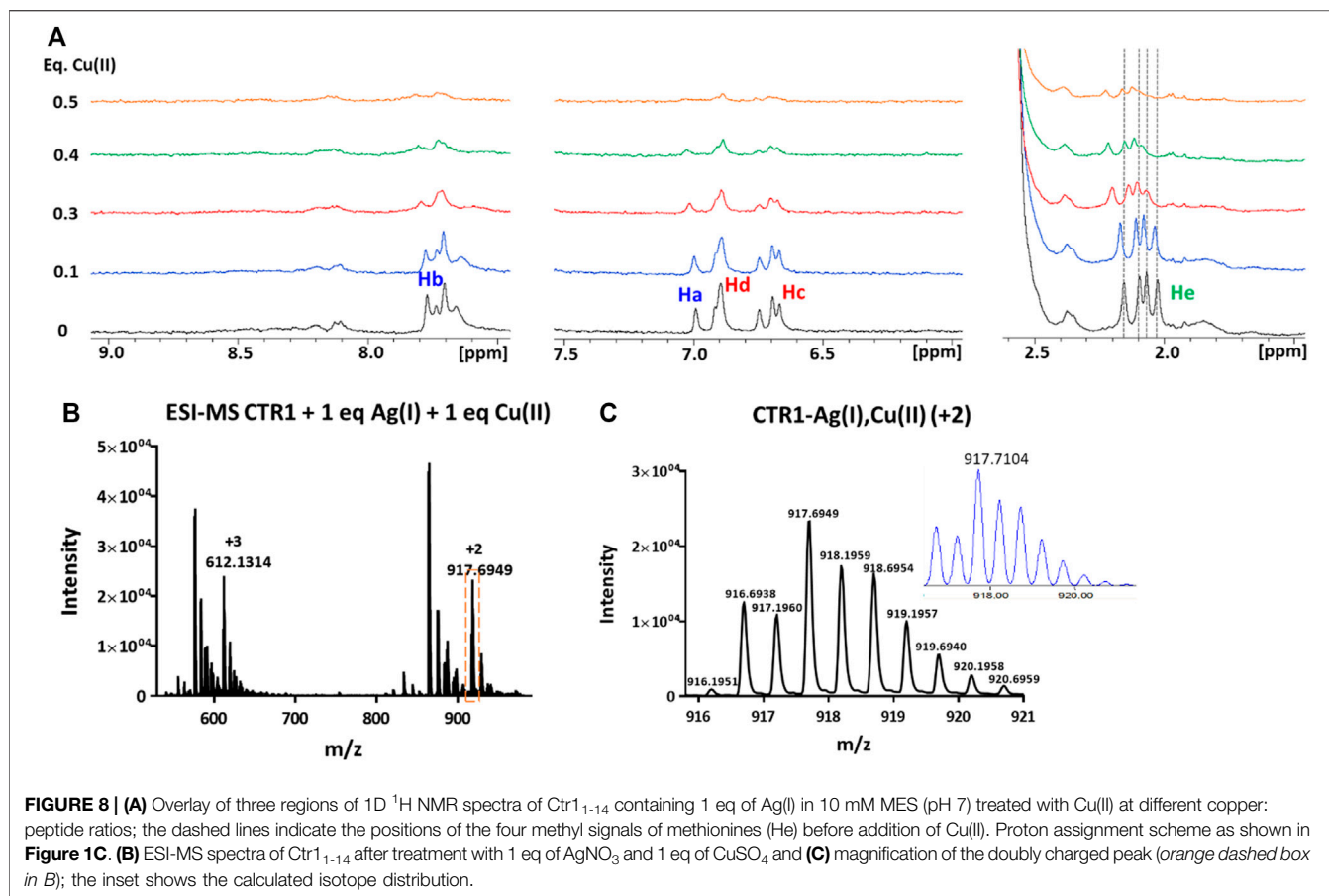
**TABLE 2** | Coordination parameters derived from the optimized coordinates in gas phase. Distances are reported interatomic distances (in Angstroms) and angles (in degrees) are defined by the atom names (peptide residues are indicated in brackets).

Distances (Å)				Angles (°)			
<b>Model 1</b>							
(Met7) Sδ-Ag(I)	(Met12) Sδ-Ag(I)	(Met7) O-Ag(I)		(Met7)Sδ-Ag(I)- (Met12)Sδ	(Met7)Sδ-Ag(I)- (Met7)O	(Met12)Sδ-Ag(I)- (Met7)O	
2.57	2.58	2.43		153.7	98.1	105.1	
<b>Model 2</b>							
(His5) Nε2-Ag(I)	(Met12) Sδ-Ag(I)	(Ser10) O-Ag(I)	(Tyr11) O-Ag(I)	(His5)Nε2-Ag(I)- (Met12)Sδ	(His5)Nε2-Ag(I)- (Ser10)O	(Met12)Sδ-Ag(I)- (Tyr11)O	(Ser10)O-Ag(I)- (Tyr11)O
2.27	2.57	2.58	2.53	149.7	112.1	110.3	72.4
<b>Model 3</b>							
(His5) Nε2-Ag(I)	(His6) Nε2-Ag(I)	(Met7) Sδ-Ag(I)	(His6) O-Ag(I)	(His5)Nε2-Ag(I)- (His6)Nε2	(His6)Nε2-Ag(I)- (Met7)Sδ	(Met7)Sδ-Ag(I)- (His6)O	(His6)O-Ag(I)- (His5)Nε2-
2.34	2.45	2.66	2.94	121.5	107.1	82.8	74.9
<b>Model 4</b>							
(His5) Nε2-Ag(I)	(His6) Nε2-Ag(I)			(His5)Nε2-Ag(I)- (His6)Nε2			
2.26	2.27			115.0			

**TABLE 3** | PBE/DGDZVP relative energies computed for all investigated models in gas phase.

	ΔE(kcal/mol)
Model 1	0.00
Model 2	0.47
Model 3	0.82
Model 4	6.33

The formation of a heterobimetallic complex of Ctr<sub>1-14</sub> with Cu(II) and Ag(I) was confirmed by the ESI-MS spectrum recorded in NH<sub>4</sub>OAc, which shows, after addition of 1 eq of CuSO<sub>4</sub> to the solution of Ctr<sub>1-14</sub> containing 1 eq of AgNO<sub>3</sub> in MES (pH 7.0), a pair of signals at 917.6949 and 612.1314 m/z (2+ and 3+ fragments, respectively), corresponding to the adduct of Ctr<sub>1-14</sub> with both Ag(I) and Cu(II), as also confirmed by the full agreement between the experimental and the theoretical isotopic



distribution patterns (**Figure 8**). A similar result was obtained when the order of salt addition was reversed (addition of AgNO<sub>3</sub> to a solution of Ctr1<sub>1-14</sub> containing 1 eq of CuSO<sub>4</sub>).

## Interaction of Ctr1<sub>1-14</sub> With Metal Ions at Low pH

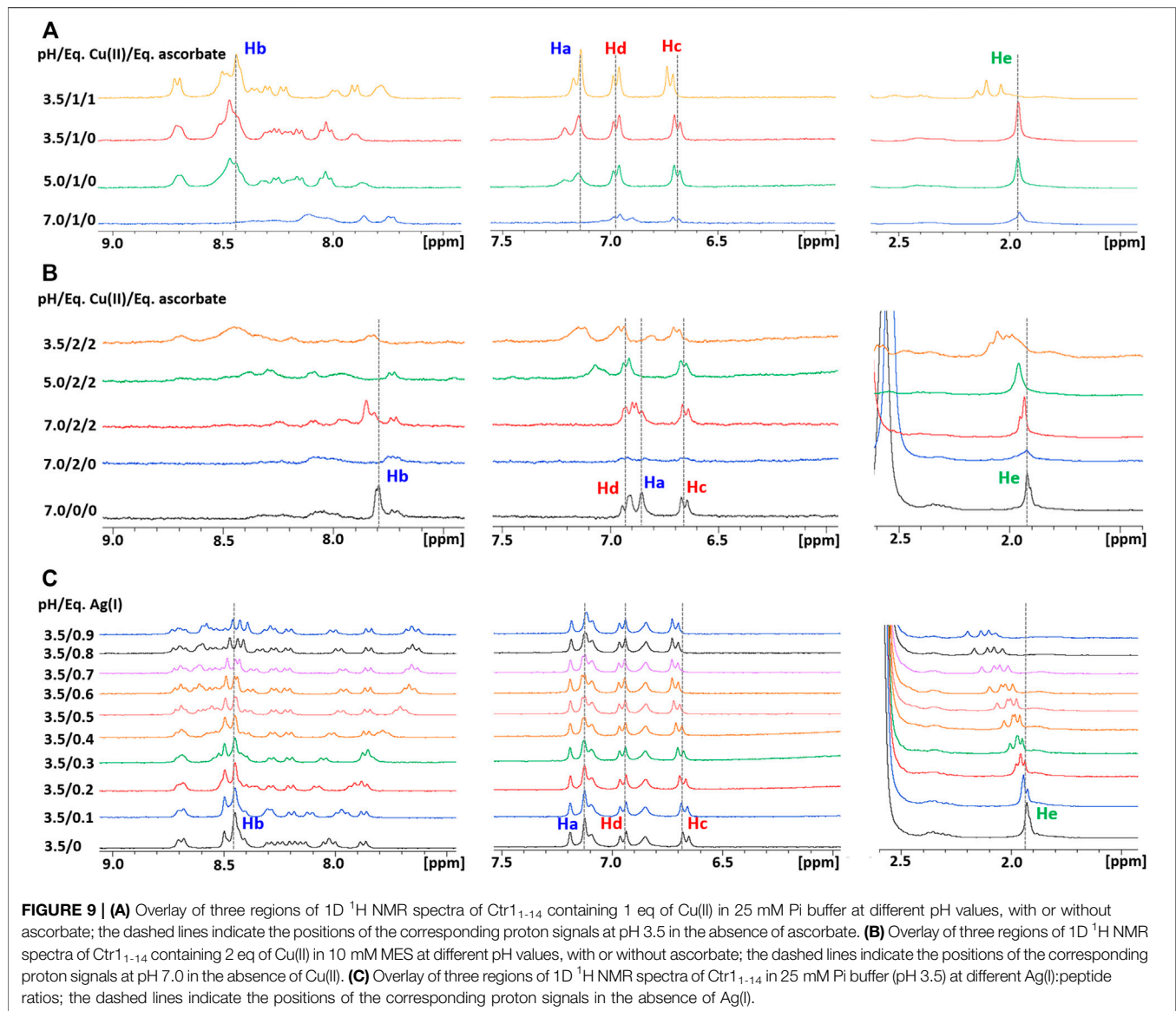
In accord with the species distribution diagram of the Cu(II) complexes with Ctr1<sub>1-14</sub>, indicating that the affinity of Cu(II) for the peptide drops at low pH due to  $\alpha$ -NH<sub>2</sub> and His protonation (Magri et al., 2022), the NMR spectra of Ctr1<sub>1-14</sub> containing 1 eq of Cu(II) in 25 mM Pi buffer show almost complete recovery of the free peptide signals when the pH is lowered from 7.0 to 3.5 (**Figure 9A**). The ESI-MS spectra at low pH of a solution of Ctr1<sub>1-14</sub> containing 1 eq of CuSO<sub>4</sub> confirmed that the Cu(II) ion is detached and only the apo-peptide is present (**Supplementary Figure S3**).

Unlike Cu(II), Ag(I) remains coordinated to Ctr1<sub>1-14</sub> also at low pH. This was shown by titration of apoCtr1<sub>1-14</sub> with AgNO<sub>3</sub> in Pi buffer at pH 3.5. In this acidic environment, Ag(I) addition causes shift and splitting of the  $\epsilon$ -CH<sub>3</sub> signals of methionines, while the His signals remain unperturbed, consistent with the imidazole nitrogens remaining protonated. It was observed also a distinct shift of the tyrosine ring protons (Hc), which may reflect the formation of a macrochelate (including Tyr11) consequent to the binding of Ag(I) to methionines (**Figure 9C**). The binding of

Ag(I) to the peptide at acidic pH was confirmed by the ESI-MS experiment performed on a solution of Ctr1<sub>1-14</sub> containing 1 eq of AgNO<sub>3</sub> at pH 3.5. The observation of the pair of signals at 887.2496 and 591.8346 m/z indicates the presence of the Ctr1<sub>1-14</sub>-Ag(I) adduct (2+ and 3+ charged fragments, respectively; **Supplementary Figure S3**).

## Susceptibility of Cu(II) to Undergo Reduction by Ascorbate

Addition of ascorbate to a neutral solution containing Cu(II) and Ctr1<sub>1-14</sub> in 1:1 ratio does not cause an appreciable reduction of Cu(II) to Cu(I); in contrast, under acidic conditions (pH 3.5), Cu(II) can be fully reduced by addition of a stoichiometric amount of ascorbate. The formation of Cu(I), consequent to the addition of ascorbate, causes a splitting of the initially degenerate signals of the four  $\epsilon$ -CH<sub>3</sub> groups of methionines (all resonating at  $\sim$ 1.95 ppm in apoCtr1<sub>1-14</sub> both under neutral and acidic conditions) into three peaks that are shifted to lower field and integrate for 3, 6, and 3H, respectively. Furthermore, the proton signals of the imidazoles do not undergo any change upon addition of ascorbate, indicating that His residues are not involved in Cu(I) binding at low pH. It can be concluded that, at pH 3.5, the formed Cu(I) ion coordinates to the sulfur atoms of methionines, as already observed for Ag(I).



In a final experiment, Ctr1<sub>1-14</sub> was loaded with two equivalents of Cu(II) ions in MES at pH 7.0 and then treated with ascorbate. In this case, ascorbate was able to reduce some Cu(II) to Cu(I), even at neutral pH, causing a partial recovery in intensity of the NMR peaks, which showed a downfield shift of His aromatic signals not observed in the solution of Ctr1<sub>1-14</sub> containing 1 eq of Cu(II) at pH 7.0. When the pH was lowered from 7.0 to 3.5, the  $\epsilon\text{-CH}_3$  signals of Met residues underwent a downfield shift indicative of Cu(I) switching from His to Met coordination (Figure 9B). It can be concluded that the second Cu(II) is more loosely bound to the peptide and can be reduced to Cu(I) by ascorbate at neutral pH and the formed monovalent copper ion coordinates to histidines at neutral pH and to methionines at low pH.

Concerning similarities and differences between Cu(I) and Ag(I) binding to Ctr1<sub>1-14</sub>, information can be drawn from the following observations. At pH 3.5, comparison between the  $^1\text{H}$

NMR spectra of 1:1 complexes of Ctr1<sub>1-14</sub> with Cu(I) and Ag(I) (top spectra of Figures 9A, C) indicates a more pronounced downfield shift of methionine-methyl signals in the case of Ag(I) with respect to Cu(I). At neutral pH, the comparison between the spectra of Ctr1<sub>1-14</sub> with Cu(I) and Ag(I) (middle spectra of Figure 9B; Figure 5) suggests that while Cu(I) preferentially binds to the bis-His motif, Ag(I) binds also to Met residues. Both observations are consistent with the softer character of Ag(I), which causes this metal ion to prefer coordination to sulfur over nitrogen.

## CONCLUSION

The present investigation highlights the ability of the first 14 residues of hCtr1 to host both divalent and monovalent metal ions and to form, beyond monometallic species, also

bimetallic complexes, such as Ctr1<sub>1-14</sub>-2Cu(II) and Ctr1<sub>1-14</sub>-2Ag(I).

Regarding the relative affinity of Cu(II) and Ag(I) ions for the peptide under neutral conditions, the ESI-MS peak intensity diagrams (**Figure 4E**; **Figure 6E**) indicate that, while the apo-peptide peaks disappear after addition of 1 eq of Cu(II), the apo-peptide is still the prevailing species after addition of 1 eq of Ag(I). Although, in general, the intensity of the ESI-MS peaks cannot be taken as a measure of the abundance of species in solution, in the present case the observed trend in intensities of the ESI-MS peaks parallels the relative abundances observed in a potentiometric investigation of Ctr1<sub>1-14</sub> solutions treated with either Cu(II) or Ag(I) ions (Magri et al., 2022). Moreover, the results are in agreement with isothermal calorimetry data for the titration with Cu(II) or Ag(I) of the entire hCtr1 ectodomain (Ctr1<sub>1-55</sub>) (Du et al., 2013).

By lowering the pH, the Cu(II) ion detaches from the peptide; in contrast the Ag(I) complex can survive in acidic conditions (pH 3.5), but shifts from histidines to methionine-only coordination.

Addition of ascorbate to a neutral solution containing Cu(II) and Ctr1<sub>1-14</sub> in 1:1 ratio does not cause an appreciable reduction of Cu(II) to Cu(I), indicating a tight binding of Cu(II) to the peptide at the ATCUN site. However, by lowering the pH to 3.5, the Cu(II) detaches from the peptide (as discussed above) and becomes susceptible to reduction to Cu(I) by ascorbate. It is noteworthy that, unlike Cu(II), Cu(I) remains coordinated to the peptide (NMR shift and splitting of the methyls of methionines), possibly by adopting a ligand coordination similar to that observed for Ag(I) at low pH and involving only Met residues (Ag(I) mode of coordination also supported by DFT calculations; **Figure 7**).

As stated above, Ctr1<sub>1-14</sub> can also bind two Cu(II) ions, but these Cu(II) ions proved to have different susceptibility to reduction by ascorbate at neutral pH. Therefore, addition of ascorbate to Ctr1<sub>1-14</sub>-2Cu(II) at pH 7.0 causes a partial recovery in intensity of the NMR signals (otherwise heavily broadened by paramagnetic Cu(II)) accompanied by an evident shift of His signals (as compared to the apo-peptide) with only a slight variation of Met signals, which is indicative of Cu(I) binding to the HH(M) site. By lowering the pH to 3.5, all Met signals undergo a downfield shift, in accord with Cu(I) shifting from HH(M) to Met-only coordination (and the detachment of the Cu(II) ion). This pH-regulated ligand switching is similar to that previously observed for the luminal HM loop of ATP7A, a human Cu(I)-transporting ATPase that shuttles between the Golgi organelle and the plasma membrane (Kline et al., 2016).

## REFERENCES

- Abraham, L., and van der Spoel, H. (2020). *GROMACS 2020.2 Source Code*. Version 2020.2. Geneva, Switzerland: CERN Data Center.
- Arnesano, F., Banci, L., and Piccioli, M. (2005). NMR Structures of Paramagnetic Metalloproteins. *Quart. Rev. Biophys.* 38, 167–219. doi:10.1017/S0033583506004161
- Baker, Z. N., Cobine, P. A., and Leary, S. C. (2017). The Mitochondrion: A Central Architect of Copper Homeostasis. *Metalomics* 9, 1501–1512. doi:10.1039/c7mt00221a
- Boal, A. K., and Rosenzweig, A. C. (2009). Structural Biology of Copper Trafficking. *Chem. Rev.* 109, 4760–4779. doi:10.1021/cr900104z
- Bossak, K., Drew, S. C., Stefaniak, E., Płonka, D., Bonna, A., and Bal, W. (2018). The Cu(II) Affinity of the N-Terminus of Human Copper Transporter CTR1: Comparison of Human and Mouse Sequences. *J. Inorg. Biochem.* 182, 230–237. doi:10.1016/j.jinorgbio.2018.01.011
- Clifford, R. J., Maryon, E. B., and Kaplan, J. H. (2016). Dynamic Internalization and Recycling of a Metal Ion Transporter: Cu Homeostasis and hCTR1, the Human Cu Uptake System. *J. Cell Sci.* 129, 1711–1721. doi:10.1242/jcs.173351
- Dancis, A., Yuan, D. S., Haile, D., Askwith, C., Eide, D., Moehle, C., et al. (1994). Molecular Characterization of a Copper Transport Protein in *S. cerevisiae*: An

That at neutral pH the N-terminal region of hCtr1 can simultaneously host a Cu(II) and a Cu(I) ion at different sites is also supported by the observation that a heterobimetallic complex (Ctr1<sub>1-14</sub>-Cu(II),Ag(I)) can be obtained by addition of Ag(I) (a mimic of Cu(I)) to a solution of Ctr1<sub>1-14</sub> already loaded with Cu(II). Interestingly, the same product is obtained by addition of Cu(II) to a solution of Ctr1<sub>1-14</sub> loaded with Ag(I).

## DATA AVAILABILITY STATEMENT

The original contributions presented in the study are included in the article/**Supplementary Material**, further inquiries can be directed to the corresponding author.

## AUTHOR CONTRIBUTIONS

FA, GN, and AP planned the experiments and the calculations. MN, AB, and FA performed the experiments. MF and AP performed the calculations. MN, AB, FA, MF, and AP analyzed the data. MN, FA, GN, and AP wrote the manuscript.

## FUNDING

This work was supported by the Italian Ministero dell'Istruzione, dell'Università e della Ricerca (Project "ICHEMFLY" PRIN 2017WBZFHL).

## ACKNOWLEDGMENTS

The authors thank the Universities of Bari, Catania and Catanzaro for support, and the Consorzio Interuniversitario di Ricerca in Chimica dei Metalli nei Sistemi Biologici (CIRCMSB). We thank Tony Laera for his valuable contribution in sample preparation and NMR spectra analysis.

## SUPPLEMENTARY MATERIAL

The Supplementary Material for this article can be found online at: <https://www.frontiersin.org/articles/10.3389/fmolb.2022.897621/full#supplementary-material>

- Unexpected Role for Copper in Iron Transport. *Cell* 76, 393–402. doi:10.1016/0092-8674(94)90345-X
- Daura, X., Gademann, K., Jaun, B., Seebach, D., van Gunsteren, W. F., and Mark, A. E. (1999). Peptide Folding: When Simulation Meets Experiment. *Angew. Chem. Int. Ed.* 38, 236–240. doi:10.1002/(sici)1521-3773(19990115)38:1/2<236::aid-anie236>3.0.co;2-m
- De Feo, C. J., Aller, S. G., Siluva, G. S., Blackburn, N. J., and Unger, V. M. (2009). Three-dimensional Structure of the Human Copper Transporter hCTR1. *Proc. Natl. Acad. Sci. U.S.A.* 106, 4237–4242. doi:10.1073/pnas.0810286106
- Du, X., Li, H., Wang, X., Liu, Q., Ni, J., and Sun, H. (2013). Kinetics and Thermodynamics of Metal Binding to the N-Terminus of a Human Copper Transporter, hCTR1. *Chem. Commun.* 49, 9134. doi:10.1039/c3cc45360j
- Ernzerhof, M., and Perdew, J. P. (1998). Generalized Gradient Approximation to the Angle- and System-Averaged Exchange Hole. *J. Chem. Phys.* 109, 3313–3320. doi:10.1063/1.476928
- Field, L. S., Luk, E., and Culotta, V. C. (2002). Copper Chaperones: Personal Escorts for Metal Ions. *J. Bioenerg. Biomembr.* 34, 373–379. doi:10.1023/a:1021202119942
- Frisch, M. J., Trucks, G. W., Schlegel, H. B., Scuseria, G. E., Robb, M. A., Cheeseman, J. R., et al. (2016). *Gaussian 16, Revision C.01*. Wallingford CT: Gaussian, Inc.,
- Galler, T., Lebrun, V., Raibaut, L., Faller, P., and Wezinfeld, N. E. (2020). How Trimerization of CTR1 N-Terminal Model Peptides Tunes Cu-Binding and Redox-Chemistry. *Chem. Commun.* 56, 12194–12197. doi:10.1039/D0CC04693K
- Georgatsou, E., Mavrogianis, L. A., Fragiadakis, G. S., and Alexandraki, D. (1997). The Yeast Fre1p/Fre2p Cupric Reductases Facilitate Copper Uptake and Are Regulated by the Copper-Modulated Mac1p Activator. *J. Biol. Chem.* 272, 13786–13792. doi:10.1074/jbc.272.21.13786
- Godbout, N., Salahub, D. R., Andzelm, J., and Wimmer, E. (1992). Optimization of Gaussian-type Basis Sets for Local Spin Density Functional Calculations. Part I. Boron through Neon. Optimization Technique and Validation. *Can. J. Chem.* 70, 560–571. doi:10.1139/v92-079
- Gonzalez, P., Bossak, K., Stefaniak, E., Hureau, C., Raibaut, L., Bal, W., et al. (2018). N-Terminal Cu-Binding Motifs (Xxx-Zzz-His, Xxx-His) and Their Derivatives: Chemistry, Biology and Medical Applications. *Chem. Eur. J.* 24, 8029–8041. doi:10.1002/chem.201705398
- Guo, Y., Smith, K., Lee, J., Thiele, D. J., and Petris, M. J. (2004). Identification of Methionine-Rich Clusters That Regulate Copper-Stimulated Endocytosis of the Human Ctr1 Copper Transporter. *J. Biol. Chem.* 279, 17428–17433. doi:10.1074/jbc.M401493200
- Haas, K. L., Putterman, A. B., White, D. R., Thiele, D. J., and Franz, K. J. (2011). Model Peptides Provide New Insights into the Role of Histidine Residues as Potential Ligands in Human Cellular Copper Acquisition via Ctr1. *J. Am. Chem. Soc.* 133, 4427–4437. doi:10.1021/ja108890c
- Hassett, R., and Kosman, D. J. (1995). Evidence for Cu(II) Reduction as a Component of Copper Uptake by *Saccharomyces cerevisiae*. *J. Biol. Chem.* 270, 128–134. doi:10.1074/jbc.270.1.128
- Himes, R. A., Park, G. Y., Barry, A. N., Blackburn, N. J., and Karlin, K. D. (2007). Synthesis and X-Ray Absorption Spectroscopy Structural Studies of Cu(I) Complexes of Histidyl-Histidine Peptides: The Predominance of Linear 2-coordinate Geometry. *J. Am. Chem. Soc.* 129, 5352–5353. doi:10.1021/ja0708013
- Hu, V. W., Chan, S. I., and Brown, G. S. (1977). X-ray Absorption Edge Studies on Oxidized and Reduced Cytochrome C Oxidase. *Proc. Natl. Acad. Sci. U.S.A.* 74, 3821–3825. doi:10.1073/pnas.74.9.3821
- Huffman, D. L., and O'Halloran, T. V. (2001). Function, Structure, and Mechanism of Intracellular Copper Trafficking Proteins. *Annu. Rev. Biochem.* 70, 677–701. doi:10.1146/annurev.biochem.70.1.677
- Ivani, I., Dans, P. D., Noy, A., Pérez, A., Faustino, I., Hospital, A., et al. (2016). Parmbsc1: a Refined Force Field for DNA Simulations. *Nat. Methods* 13, 55–58. doi:10.1038/nmeth.3658
- Jiang, J., Nadas, I. A., Kim, M. A., and Franz, K. J. (2005). A Mets Motif Peptide Found in Copper Transport Proteins Selectively Binds Cu(I) with Methionine-Only Coordination. *Inorg. Chem.* 44, 9787–9794. doi:10.1021/ic051180m
- Jorgensen, W. L., Chandrasekhar, J., Madura, J. D., Impey, R. W., and Klein, M. L. (1983). Comparison of Simple Potential Functions for Simulating Liquid Water. *J. Chem. Phys.* 79, 926–935. doi:10.1063/1.445869
- Kagan, H. M., and Li, W. (2003). Lysyl Oxidase: Properties, Specificity, and Biological Roles inside and outside of the Cell. *J. Cell. Biochem.* 88, 660–672. doi:10.1002/jcb.10413
- Kline, C. D., Gambill, B. F., Mayfield, M., Lutsenko, S., and Blackburn, N. J. (2016). pH-Regulated Metal-Ligand Switching in the HM Loop of ATP7A: A New Paradigm for Metal Transfer Chemistry. *Metallomics* 8, 729–733. doi:10.1039/C6MT00062B
- Lee, J., Prohaska, J. R., and Thiele, D. J. (2001). Essential Role for Mammalian Copper Transporter Ctr1 in Copper Homeostasis and Embryonic Development. *Proc. Natl. Acad. Sci. U.S.A.* 98, 6842–6847. doi:10.1073/pnas.111058698
- Lutsenko, S. (2021). Dynamic and Cell-Specific Transport Networks for Intracellular Copper Ions. *J. Cell Sci.* 134, jcs240523. doi:10.1242/jcs.240523
- Magri, A., Tabbi, G., Naletova, I., Attanasio, F., Arena, G., and Rizzarelli, E. (2022). A Deeper Insight in Metal Binding to the hCtr1 N-Terminus Fragment: Affinity, Speciation and Binding Mode of Binuclear Cu<sup>2+</sup> and Mononuclear Ag<sup>+</sup> Complex Species. *Ijms* 23, 2929. doi:10.3390/ijms23062929
- Matoba, Y., Kumagai, T., Yamamoto, A., Yoshitsu, H., and Sugiyama, M. (2006). Crystallographic Evidence that the Dinuclear Copper Center of Tyrosinase Is Flexible during Catalysis. *J. Biol. Chem.* 281, 8981–8990. doi:10.1074/jbc.M509785200
- Molloy, S. A., and Kaplan, J. H. (2009). Copper-dependent Recycling of hCTR1, the Human High Affinity Copper Transporter. *J. Biol. Chem.* 284, 29704–29713. doi:10.1074/jbc.M109.000166
- Nevitt, T., Öhrvik, H., and Thiele, D. J. (2012). Charting the Travels of Copper in Eukaryotes from Yeast to Mammals. *Biochim. Biophys. Acta (BBA) - Mol. Cell Res.* 1823, 1580–1593. doi:10.1016/j.bbamcr.2012.02.011
- O'Halloran, T. V., and Culotta, V. C. (2000). Metallochaperones, an Intracellular Shuttle Service for Metal Ions. *J. Biol. Chem.* 275, 25057–25060. doi:10.1074/jbc.R000006200
- Ohgami, R. S., Campagna, D. R., McDonald, A., and Fleming, M. D. (2006). The Steap Proteins Are Metalloreductases. *Blood* 108, 1388–1394. doi:10.1182/blood-2006-02-003681
- Oosterheert, W., van Bezouwen, L. S., Rodenburg, R. N. P., Granneman, J., Förster, F., Mattevi, A., et al. (2018). Cryo-EM Structures of Human STEAP4 Reveal Mechanism of Iron(III) Reduction. *Nat. Commun.* 9, 4337. doi:10.1038/s41467-018-06817-7
- Palumaa, P. (2013). Copper Chaperones. The Concept of Conformational Control in the Metabolism of Copper. *FEBS Lett.* 587, 1902–1910. doi:10.1016/j.febslet.2013.05.019
- Petris, M. J., Smith, K., Lee, J., and Thiele, D. J. (2003). Copper-stimulated Endocytosis and Degradation of the Human Copper Transporter, hCtr1. *J. Biol. Chem.* 278, 9639–9646. doi:10.1074/jbc.M209455200
- Petersen, E. F., Goddard, T. D., Huang, C. C., Couch, G. S., Greenblatt, D. M., Meng, E. C., et al. (2004). UCSF Chimera? A Visualization System for Exploratory Research and Analysis. *J. Comput. Chem.* 25, 1605–1612. doi:10.1002/jcc.20084
- Pfaendtner, J., and Bonomi, M. (2015). Efficient Sampling of High-Dimensional Free-Energy Landscapes with Parallel Bias Metadynamics. *J. Chem. Theory Comput.* 11, 5062–5067. doi:10.1021/acs.jctc.5b00846
- Pope, C. R., Flores, A. G., Kaplan, J. H., and Unger, V. M. (2012). Structure and Function of Copper Uptake Transporters. *Curr. Top. Membrin.* 69, 97–112. doi:10.1016/B978-0-12-394390-3.00004-5
- Prigge, S. T., Mains, R. E., Eipper, B. A., and Amzel\*, L. M. (2000). New Insights into Copper Monooxygenases and Peptide Amidation: Structure, Mechanism and Function. *Cell. Mol. Life Sci.* 57, 1236–1259. doi:10.1007/PL00000763
- Pushie, M. J., Shaw, K., Franz, K. J., Shearer, J., and Haas, K. L. (2015). Model Peptide Studies Reveal a Mixed Histidine-Methionine Cu(I) Binding Site at the N-Terminus of Human Copper Transporter 1. *Inorg. Chem.* 54, 8544–8551. doi:10.1021/acs.inorgchem.5b01162
- Ren, F., Logeman, B. L., Zhang, X., Liu, Y., Thiele, D. J., and Yuan, P. (2019). X-ray Structures of the High-Affinity Copper Transporter Ctr1. *Nat. Commun.* 10, 1386. doi:10.1038/s41467-019-09376-7
- Robinson, N. J., and Winge, D. R. (2010). Copper Metallochaperones. *Annu. Rev. Biochem.* 79, 537–562. doi:10.1146/annurev-biochem-030409-143539
- Rubino, J. T., Riggs-Gelasco, P., and Franz, K. J. (2010). Methionine Motifs of Copper Transport Proteins Provide General and Flexible Thioether-Only

- Binding Sites for Cu(I) and Ag(I). *J. Biol. Inorg. Chem.* 15, 1033–1049. doi:10.1007/s00775-010-0663-9
- Santoro, A., Walke, G., Vileno, B., Kulkarni, P. P., Raibaut, L., and Faller, P. (2018). Low Catalytic Activity of the Cu(II)-binding Motif (Xxx-Zzz-His; ATCUN) in Reactive Oxygen Species Production and Inhibition by the Cu(i)-Chelator BCS. *Chem. Commun.* 54, 11945–11948. doi:10.1039/c8cc06040a
- Shearer, J., and Szalai, V. A. (2008). The Amyloid- $\beta$  Peptide of Alzheimer's Disease Binds Cu<sup>1+</sup> in a Linear Bis-His Coordination Environment: Insight into a Possible Neuroprotective Mechanism for the Amyloid- $\beta$  Peptide. *J. Am. Chem. Soc.* 130, 17826–17835. doi:10.1021/ja805940m
- Siiskonen, A., and Priimagi, A. (2017). Benchmarking DFT Methods with Small Basis Sets for the Calculation of Halogen-Bond Strengths. *J. Mol. Model.* 23, 50. doi:10.1007/s00894-017-3212-4
- Tsukihara, T., Aoyama, H., Yamashita, E., Tomizaki, T., Yamaguchi, H., Shinzawa-Itōh, K., et al. (1995). Structures of Metal Sites of Oxidized Bovine Heart Cytochrome C Oxidase at 2.8 Å. *Science* 269, 1069–1074. doi:10.1126/science.7652554
- Van Den Berghe, P. V. E., Folmer, D. E., Malingré, H. E. M., Van Beurden, E., Klomp, A. E. M., Van De Sluis, B., et al. (2007). Human Copper Transporter 2 Is Localized in Late Endosomes and Lysosomes and Facilitates Cellular Copper Uptake. *Biochem. J.* 407, 49–59. doi:10.1042/BJ20070705
- Yang, Y., Zhu, Y., Hu, H., Cheng, L., Liu, M., Ma, G., et al. (2019). Cuprous Binding Promotes Interaction of Copper Transport Protein hCTR1 with Cell Membranes. *Chem. Commun.* 55, 11107–11110. doi:10.1039/C9CC04859F
- Zhou, B., and Gitschier, J. (1997). hCTR1: A Human Gene for Copper Uptake Identified by Complementation in Yeast. *Proc. Natl. Acad. Sci. U.S.A.* 94, 7481–7486. doi:10.1073/pnas.94.14.7481
- Conflict of Interest:** The authors declare that the research was conducted in the absence of any commercial or financial relationships that could be construed as a potential conflict of interest.
- Publisher's Note:** All claims expressed in this article are solely those of the authors and do not necessarily represent those of their affiliated organizations, or those of the publisher, the editors and the reviewers. Any product that may be evaluated in this article, or claim that may be made by its manufacturer, is not guaranteed or endorsed by the publisher.
- Copyright © 2022 Nardella, Fortino, Barbanente, Natile, Pietropaolo and Arnesano. This is an open-access article distributed under the terms of the Creative Commons Attribution License (CC BY). The use, distribution or reproduction in other forums is permitted, provided the original author(s) and the copyright owner(s) are credited and that the original publication in this journal is cited, in accordance with accepted academic practice. No use, distribution or reproduction is permitted which does not comply with these terms.